Remediation Journal

WILEY

RESEARCH ARTICLE OPEN ACCESS

Co-Application of Wood Biochar and Nano-Titanium Dioxide to Immobilize Vanadium in Alkaline Soils

Melissa R. Haak[1] | Srimathie P. Indraratne[1] | Chammi P. Attanayake[2] | Douglas M. Goltz[3] | Daniel M. Applin[4]

[1]Department of Environmental Studies and Sciences, The University of Winnipeg, Winnipeg, Manitoba, Canada | [2]Institute for Sustainability, Energy, and Environment, University of Illinois Urbana-Champaign, Urbana, Illinois, USA | [3]Department of Chemistry, The University of Winnipeg, Winnipeg, Manitoba, Canada | [4]Department of Geography, The University of Winnipeg, Winnipeg, Manitoba, Canada

Correspondence: Srimathie P. Indraratne (s.indraratne@uwinnipeg.ca)

Received: 1 July 2024 | **Revised:** 13 November 2024 | **Accepted:** 14 November 2024

Funding: This research was financially supported by the Natural Sciences and Engineering Research Council of Canada—Discovery Development Grant (NSERC-DDG, S.P. Indraratne).

Keywords: alkaline soil | biochar | mobile fraction | pH-adsorption edge | titanium dioxide nanoparticles

ABSTRACT

Titanium dioxide (TiO_2) and biochar have been used as amendments to adsorb vanadium (V) in aqueous solutions; however, their simultaneous application in the remediation of V-contaminated neutral-alkaline soils is rare. TiO_2 nanoparticles, biochar, and a blend of biochar+TiO_2 were investigated as amendments for an alkaline V-contaminated soil. Treatments involved mixing (weight basis) 1% TiO_2 (T1), 5% biochar (T2), 1% TiO_2 + 5% biochar (T3) with soil, and an unamended soil (T4). An adsorption edge study was performed from pH 4 to 10 at the V concentration of 200 mg L^{-1}. A standard vanadium (V) solution was prepared using $NaVO_3$. An incubation study was conducted over 3 months with V-contaminated soil at a rate of 200 mg kg^{-1}, at 80% field capacity. At the end of the incubation period, the treated soils were subjected to V fractionation. X-ray diffraction (XRD) patterns and FTIR spectra of TiO_2 nanoparticles, biochar, uncontaminated soil, and four treated soils were obtained. The adsorption edge of V was below pH 4.6, suggesting reduced retention of V in alkaline soils. In the combined treatment, the adsorption edge was elevated by one unit compared to the control. V adsorption increased in TiO_2, biochar, and combined TiO_2+biochar treatments at 7%, 4%, and 20%, respectively, compared with the unamended soil (control) at a pH of ~7.6. Functional groups revealed the possibility of inner-sphere and outer-sphere adsorption mechanisms between vanadate and the mix amendment of TiO_2+biochar. The labile V fraction decreased, and the nonlabile V fraction increased, significantly in the TiO_2+biochar amended soil compared to the unamended soil. Applying a blend of biochar+TiO_2 reduced the mobility of V in a neutral-alkaline soil, thereby preventing it from contaminating the nearby soil and water bodies.

1 | Introduction

Vanadium (V) is a potentially toxic element (PTE) gaining attention because of its increased usage and toxicity. Titanomagnetite ores are considered the most abundant source of V and are mined globally, while V is also a byproduct of mining iron, steel, and phosphate ores (Imtiaz et al. 2015; Makhotkina and Shubina 2017; Zhang et al. 2011). South Africa and China have experienced severe soil contamination by V in mining and smelting regions (Haak and Indraratne 2023). Vanadium is found in oil and coal and released during fossil fuel combustion, leading to V deposition as far as 5 km away from the combustion site (Khan et al. 2011).

Abbreviations: BCR, European Community Bureau of Reference; FTIR, Fourier-transform infrared spectroscopy; ICP-AES, inductively coupled plasma-atomic emission spectroscopy; TiO_2, titanium dioxide nanoparticles; XRD, X-ray diffraction spectrometry.

Phosphorous (P) ores containing V have led to adding V to soils via P-fertilizer application (Imtiaz et al. 2015; Molina et al. 2009).

Vanadium can become mobilized through the redox process, which solubilizes V-containing minerals, while pH affects V adsorption to the soil colloid (Chen et al. 2021; Huang et al. 2015). Vanadium (+5) is V's most soluble, mobile, and toxic species and is the most thermodynamically stable species in oxygen-rich environments (Shaheen et al. 2019). Various inorganic and organic reactions involving substances like H_2S and organic matter, as well as the activity of metal-reducing microorganisms, can reduce V^{5+} to the less soluble V^{4+} state (Lu, Johnson, and Hook 1998; Wanty and Goldhaber 1992; Zhang et al. 2015). The valence of V is sensitive to oxygen, which greatly affects its geochemical behavior and toxicity (Huang et al. 2015). Species of V^{3+} exist only in anoxic conditions and are oxidized even at low levels of O_2 (Shaheen et al. 2019). The V^{4+} species is the predominant form at pH 3–5 as the vanadyl cation VO^{2+}. Still, it is of low mobility due to the formation of strong complexes with organic substances in soil, the substitution of V^{4+} for Al^{3+} in clay minerals, and adsorption onto Fe-oxides (Hu, Yue, and Peng 2018; Reijonen, Metzler, and Hartikainen 2016). Negatively charged anions of V^{5+} (vanadates) are predominant above pH 5 in aerobic environments and have the highest mobility among the V species (Chen et al. 2021; Fei et al. 2022). Vanadate exists as $H_2VO_4^-$ from pH 5 to 7 and HVO_4^{2-} at pH 7 to 10, while at high pH VO_4^{3-} is dominant (Gustafsson 2019; Reijonen, Metzler, and Hartikainen 2016). The structure of vanadate is analogous to phosphate ($H_2PO_4^-$, HPO_4^{2-}, and PO_4^{3-}), making vanadate a potent inhibitor of phosphate-targeting enzymes, such as ATPase and phosphorylase, which is the primary reason V is toxic to organisms that rely on these enzymes (Crans et al. 2004; Kollur and Shwetha 2020). Therefore, the mobility of V in soils primarily depends on redox potential, pH, soil organic matter (SOM), microbial activities, and the presence of Fe-, Al-, and Mn-(hydr)oxides, and vanadates are the most mobile in alkaline, oxic soil conditions (Chen et al. 2021; Reijonen, Metzler, and Hartikainen 2016; Shaheen et al. 2019).

Among the most efficient remediation methods, chemical stabilization is attractive for large field sites because it does not require as much upkeep as phyto and microbial remediation, and the materials are often inexpensive (Liu et al. 2018). Biochar and metal oxides are among the most popular soil amendments. Biochar has been used in previous studies to immobilize metal(loid)s, such as Cd, As, Cr, and Cu in soils (Ahmad et al. 2018; He et al. 2019; Lomaglio et al. 2018; Mehmood et al. 2018; Weber and Quicker 2018). Studies have shown biochar successfully immobilized V within the soil matrix (El-Naggar et al. 2021; Yu et al. 2020) and these studies were conducted for acidic soils. The presence of π bonded carbons (alkenes) is favorable for the thermodynamic stability of biochar in soil environments (Weber and Quicker 2018). Biochar sourced from wood tends to have a higher abundance of carbonyl (ketones) and carboxyl groups and has a superior adsorption capacity of V compared to other feedstocks (Ahmad et al. 2018; El-Naggar et al. 2021).

Among the metal oxides, Al- and Fe-oxides are the most studied as adsorbent materials for V remediation (Peacock and Sherman 2004; Vessey et al. 2020; Abernathy et al. 2022). Titanium dioxide has been used to remove V from spent catalyst leachate and wastewater in previous studies (Naeem, Westerhoff, and Mustafa 2007; Wołowicz et al. 2022). The incorporation of metal oxides has been shown to improve the adsorption of anions by biochar because it increases the number of binding sites (Ghanim et al. 2020; Weidner et al. 2022; Yu et al. 2020). Titanium dioxide is a good option for PTE remediation because of its stability, as it is not easily reduced and is resistant to oxidation (Weidner et al. 2022). The reactive surface, the abundance of various O-containing functional groups, and the hydrophilicity of the wood biochar contributed to high V immobility in biochar-amended soils (El-Naggar et al. 2021; Weber and Quicker 2018). Therefore, the incorporation of both materials could potentially be very beneficial for immobilizing dissolved V. Although the mixed system of biochar and TiO_2 systems have previously been prepared for metal remediation in wastewater, none have been used to remediate V in soil (Weidner et al. 2022). Further, biochar has positive results in stabilizing V in acidic soils; it has rarely been tested in alkaline soils (El-Naggar et al. 2021). Therefore, the objectives of this study were to: (1) investigate the effectiveness of wood biochar, nano-TiO_2, and a mixture of both for immobilizing V in alkaline soil by comparing the V sorption capacities of the amended soil to unamended soil; and (2) elucidate V-amendment binding mechanisms using spectroscopic and fractionation studies.

2 | Materials and Methods

Sodium metavanadate ($NaVO_3$, 99.9%) and nano-titanium dioxide (TiO_2, ≥ 99.5%) were purchased from Sigma-Aldrich (Milwaukee, WI, USA). Biochar made from 100% wood was purchased from Canadian Agrichar (Char+, Maple Ridge, BC, Canada) and had a 70% carbon and 30% ash ratio. All experiments used ultrapure water (Milli-Q; 18 MΩ cm). Sodium metavanadate was used to prepare the stock solution and to conduct adsorption and incubation studies as described in previous investigations (Gäbler et al. 2009; Gan et al. 2020; Larsson, Hadialhejazi, and Gustafsson 2017; Luo et al. 2017).

2.1 | Soil and Amendment Properties

The soil was collected from Glenlea, Manitoba, Canada (Rego Black Chernozem; MAFRI 2010) at 0–15 cm depth. The soil was air-dried, homogenized, sieved through a 2 mm sieve, and stored at 20.5°C until ready for use. Important soil and amendment properties were determined, and details of the analytical methods are provided with the supplemental materials.

The soil was contaminated with $NaVO_3$ solution at 200 mg V kg^{-1} and left for 2 weeks. Treatments were prepared by mixing contaminated soil with 1% w/w nano-TiO_2 (T1), 5% w/w biochar (T2), 1% w/w nano-TiO_2 + 5% w/w biochar (T3), and unamended soil (T4) as the control. Nano oxides of Al, Si, Fe, and Ti have been proven effective in metal(loid) remediation at 1%–5% (w/w) application rates (Naderi and Jalali 2019; Indraratne et al. 2021). Biochar has also demonstrated its remediation capabilities at rates of 2.5%–5% (w/w) for metal(loid)s in soils (Zand, Tabrizi, and Heir 2020). For this study, considering

environmental health consequences, we have opted to use the lowest effective nano TiO_2 rate (1% w/w) and a field-application rate of biochar (5% w/w) to remediate V-contaminated soil.

2.2 | pH Adsorption Edge

The pH adsorption edge for V was determined for soil mixed with nano-TiO_2 (T1), biochar (T2), nano-TiO_2+biochar (T3), and soil only (T4) as described previously. A batch sorption study was conducted with varying pH ranges from 4 to 10 in triplicate for all treatments (Hu et al. 2015; Luo et al. 2017). The experiment involved placing 1 g of soil samples (T1–T4) into 50 mL falcon tubes. These samples were then shaken in a reciprocal shaker with a 0.01 M $NaNO_3$ electrolyte solution for 24 h. The samples were then contaminated with $NaVO_3$ to achieve a V concentration of 200 mg L^{-1}, and the volume was adjusted to 25 mL with 0.01 M $NaNO_3$. The pH of the samples was adjusted to their respective levels using either 0.1 M HNO_3 or 0.1 M NaOH, before the start of the shaking. The samples were shaken for 5 h, and the final pH was measured. Subsequently, the samples were centrifuged at 6000 rpm for 15 min, and the supernatant was filtered through 0.22 μm nylon filters. Samples were stored at 4°C after being acidified with 50 μL of trace metal-grade HNO_3 until the analysis. The V concentration in the supernatant was determined using inductively coupled plasma optical emission spectrometry (ICP-OES; Thermo iCAP 6500 Duo, Cambridge, UK). The adsorption edge for each treatment was determined by plotting the adsorbed V against the equilibrium pH.

The geochemical equilibrium speciation modeling software, Visual MINTEQ 3.1 (Gustafsson 2013), was used to estimate the percentage of each polyvanadate species at each pH. The concentration of V used in the adsorption edge experiment was 200 mg L^{-1}. This concentration is equivalent to 3924 μM of V. The input parameters used for the model were 0.01 M Na^+, 0.01 M NO_3^-, 3924 μM of V^{5+}, and a pH range of 4–10.

2.3 | Incubation Study and Sequential Extraction

An incubation experiment was conducted separately to investigate the suitability of biochar, TiO_2, and the mixture of both amendments in an alkaline soil of pH 7.6. A 50 g sample of each treatment (T1–T4 prepared as described above) was kept in a plastic incubation container and ultrapure water was added to maintain moisture content at 80% field capacity. Treatments were incubated for 3 months at room temperature in triplicate and the pH was measured at the beginning and the end of the incubation period. The modified sequential extraction procedure developed by the European Community Bureau of Reference (BCR) was performed at the end of the incubation period to determine the geochemical fractions of V among the treatments (Pueyo et al. 2008; Xiao et al. 2017). This procedure extracts four different fractions (F1, F2, F3, and F4) of V sequentially, and the procedure details are provided in the Supporting Information. F1 represents the exchangeable/acid-soluble fraction, F2 represents the reducible fraction, F3 represents the oxidizable fraction, and F4 represents the residual fraction (Xiao et al. 2017). The concentration of V in each of the fractions among treatments was determined using ICP-AES (ICP-AES, Thermo iCAP 6500 Duo, Cambridge, UK).

2.4 | Characterization of Amended and Unamended Soils

X-ray diffraction (XRD) was performed on four treatments (T1, T2, T3, and T4) at the end of the incubation study using slurries dried on a zero-background plate (Bruker D8 Advance, Germany). The XRD analysis involved acquiring continuous scan data (2θ) from 5 to 40° at increments of 0.02° and integration time of 1 s per step. Incident X-rays were generated from a Co X-ray tube operated at 40 kV and 40 mA, using a take-off angle at 6°.

Fourier-transform infrared spectroscopy (FTIR) was performed on biochar, nano-TiO_2, and dry samples of all four treated soils using an Alpha II Platinum FTIR spectrometer (Bruker D8 Advance, Germany). Transmittance spectra were acquired by mixing the samples in KBr pellets. For each sample, 16 spectra were acquired with 4 cm^{-1} resolution (400–4000 cm^{-1}).

2.5 | Statistical Analysis

Analysis of variance (ANOVA) for V concentrations extracted from sequential extraction procedure was performed using PROC GLIMMIX in SAS software, Version 9.4 (SAS Institute Inc 2013). **Treatment**, **Fraction**, and **Interaction** were used as fixed factors. The V concentration was modeled as the normal distribution, and the Tukey multiple comparison procedure was used to compare the least square means. Significance was determined at $\alpha = 0.05$.

3 | Results

3.1 | Initial Properties

The soil studied had an alkaline pH, a high SOM content, a calcium carbonate equivalent (CCE) closer to calcareous soil, a high cation exchange capacity, and a low salinity level (Table 1). The pH of biochar and nano-TiO_2 was alkaline and acidic, respectively. The nano-TiO_2 had a particle size of 21 nm and a surface area of 50 $m^2\,g^{-1}$ (product certificate). The total V in the soil and biochar were 161 and 29 mg kg^{-1}, respectively. The XRD patterns of nano-TiO_2 showed the characteristic diffraction peaks of anatase with d-spacings 0.35, 0.32, 0.24, and 0.19 nm (data not shown).

3.2 | Adsorption Experiments of Vanadium in Amended and Unamended Soils

The equilibrium pH versus adsorbed V was plotted for T1, T2, T3, and T4 (Figure 1). In all treatments, there was a noticeable reduction in V adsorption as the pH increased from 4 to 10. The pH adsorption edge for V in treatments T1, T2, and T4 occurred at pH < 4.6, resulting in adsorbed V amounts of 1709, 1717, and 1699 mg kg^{-1}, respectively. However, in T3, the adsorption edge

TABLE 1 | Properties of uncontaminated soil and amendments.

Property	Soil	Wood biochar	Nano-TiO_2
pH (distilled water)	7.6 (1:2.5)	9.3 (1:9)	3.6 (1:2.5)
Electrical conductivity (dS m^{-1})	0.64	0.63	ND
Organic matter (%)	7.9	74.3	ND
Calcium carbonate equivalent (CCE%)	13.6	0.25	ND
Cation exchange capacity (CEC; cmol(+) kg^{-1})	38.7	ND	ND
Total TiO_2%	0.35	0.26	> 99.5
Total V (mg kg^{-1})	161	29	BDL

Note: solid:solution ratio is given in the parenthesis.
Abbreviations: BDL, below detection limit; ND, not detected.

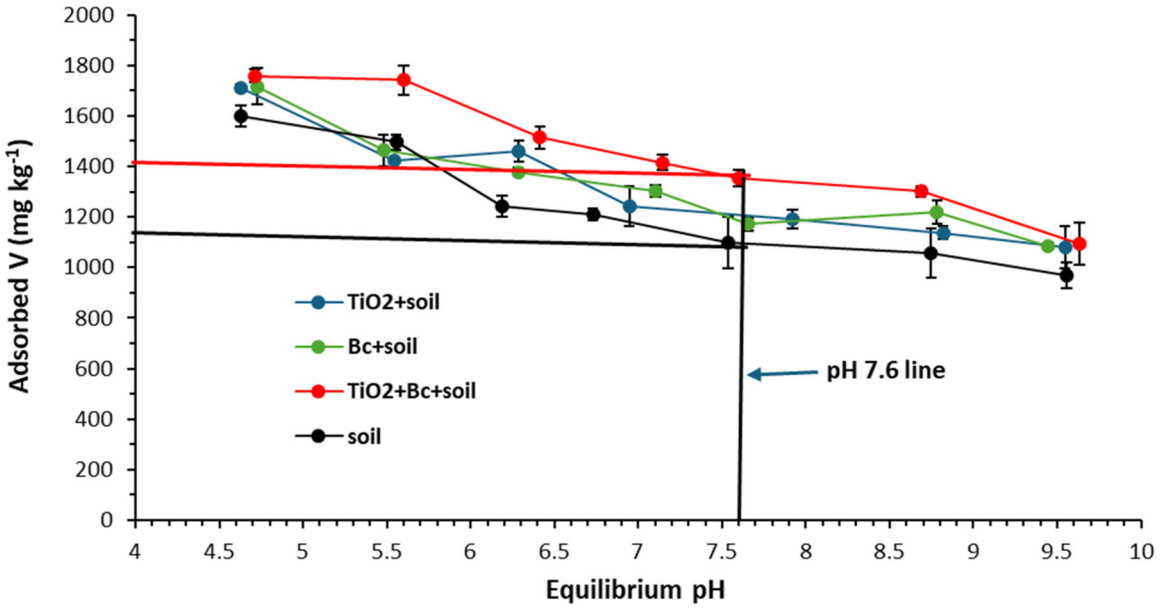

FIGURE 1 | Adsorption of V against equilibrium pH for unamended soil (control) and soil amended with TiO_2, biochar (Bc), and mix of TiO_2 and Bc (Error bars show the standard deviation of the mean, $n = 3$; vertical line indicates the soil's pH, and horizontal lines indicate the amounts adsorbed at soil's pH by the control and the mix [TiO_2 and Bc] treatment). [Color figure can be viewed at wileyonlinelibrary.com]

shifted to pH 5.6, leading to increased adsorption of V to 1741 V mg kg^{-1}. Several studies, including those by Larsson, Hadialhejazi, and Gustafsson (2017), Luo et al. (2017), and Mikkonen and Tummavuori (1994), have observed an adsorption edge ~pH 4 for various soils. Although our adsorption study covered a range from pH 4 to 10, the lowest equilibrium pH in this alkaline soil increased to ~4.6. To precisely determine the adsorption edge for T1, T2, and T4, experimenting starting from pH 3 would be more appropriate. Nevertheless, the results indicated that the combined amendment shifted the adsorption edge toward a higher pH compared to the other treatments.

The collected soil had a natural pH of 7.6, with V adsorption of 1120 mg kg^{-1}. Compared to the unamended control, soils amended with TiO_2 adsorbed 1200 mg kg^{-1}, biochar (Bc) adsorbed 1170 mg kg^{-1}, and the combined TiO_2+Bc achieved an adsorption of 1400 mg kg^{-1} (Figure 1). Therefore, V adsorption increased by 7% with TiO_2, 4% with biochar, and 20% with the combined TiO_2+Bc treatment compared to the control at the soil's natural pH.

Figure 2 illustrates the predicted percentage of each V species (including both adsorbed and dissolved) relative to the total concentration of added V. The predicted V species indicated that the preferred V species for adsorption varied with the changing equilibrium pH. Within the pH range of 4–6, polyvanadates such as $HV_{10}O_{28}^{-5}$ and $NaHV_{10}O_{28}^{-5}$ were favored. Between pH 6 and 8, species like $V_4O_{12}^{4-}$, $H_2VO_4^{-}$, and $H_2V_2O_7^{2-}$ were favored, while at pH 8–10, HVO_4^{-5} species became predominant and reached 100% dominance by pH 10 (Figure 2). Similar predictions of polyvanadate and orthovanadate V species were reported by Vessey et al. (2020) in their study conducted at 5000 μM total V. Based on the same study, it was found that the polyvanadate fraction in the aqueous solution was less than 10% when the experiment was conducted at lower V concentrations, that is, 100 μM (Vessey et al. 2020). Additionally, an EXAFS study revealed that the adsorption of polyvanadate at a 100 μM concentration of V was negligible, with noticeable adsorption observed only when the concentration of V^{5+} reached as high as 1.5 mM (Abernathy et al. 2022). Therefore, it is likely that the adsorption capacity of V in the

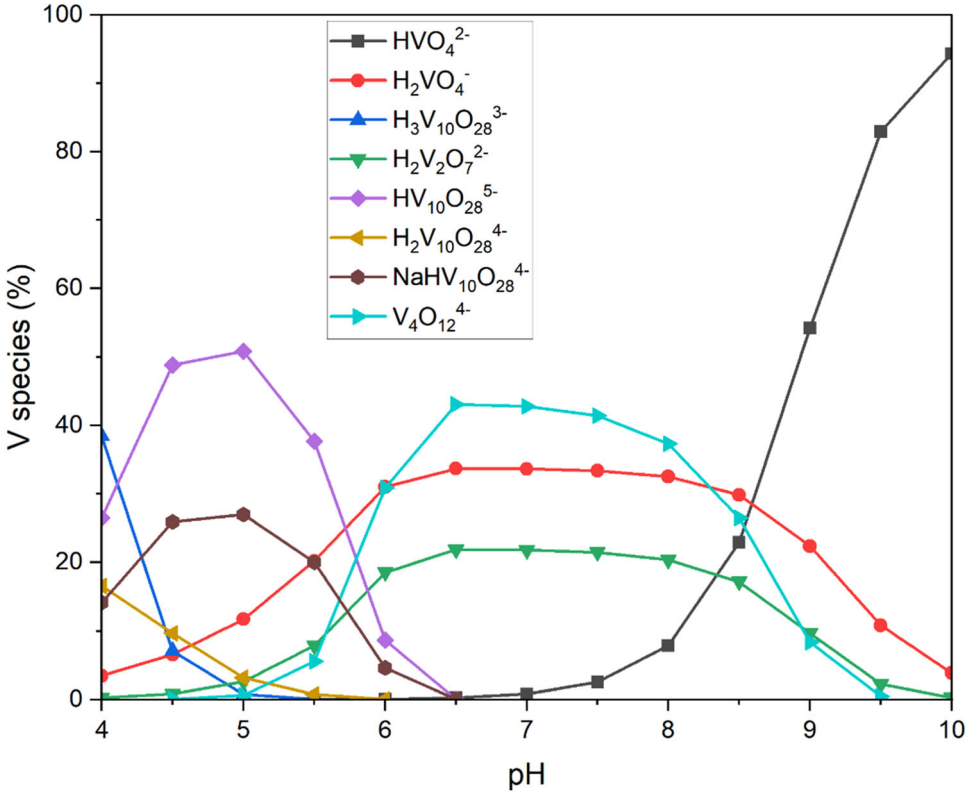

FIGURE 2 | Percentage of predicted V species (total of adsorbed and dissolved) from total concentration of V (200 mg L^{-1}) added. [Color figure can be viewed at wileyonlinelibrary.com]

adsorption experiment may have been influenced by the presence of polyvanadates at higher concentrations.

3.3 | Vanadium Fractionation in Amended and Unamended Soils

At the end of the incubation period, the pH of the amended and unamended soils varied in a narrow range. The initial pH of all treatments was ~7.6 and not significantly different. The final pH with standard error of mean were 7.60 ± 0.01 (T1), 7.68 ± 0.02 (T2), 7.69 ± 0.02 (T3), and 7.64 ± 0.01 (T4), and the values were not significantly different. Due to the high buffering capacity as expected due to the soil's OM%, CEC, and presence of $CaCO_3$, adding amendments in the given quantities (1% TiO_2 and 5% biochar) did not change the pH of the soil. Therefore, V adsorption to the amended and unamended soil occurred at ~7.6 pH, during the incubation period. Since the incubation study was conducted at the low V contamination rate (200 mg kg^{-1}), at the soil's pH ~7.6, the presence of orthovanadate species ($H_2VO_4^-$ and HVO_4^{2-}) can be expected.

The sequentially extracted V at the end of the incubation period for each treatment is shown in Figure 3. No significant difference was observed in the total concentrations of V between amended and unamended soil treatments, as calculated by combining the four fractions, namely, acid-soluble (exchangeable), reducible, oxidizable, and residual fractions (data not presented). The proportion of V separated into different operationally defined fractions using sequential fractionation in amended and unamended soils followed the order; exchangeable-V (F1) ≤ oxidizable-V (F3) < reducible-V (F2) < residual-V (F4).

Only ~1%–2.5% of the total V were found in exchangeable (F1) and oxidizable (F3) fractions and V concentrations were not significantly different among treatments in these two fractions. In contrast, reducible (F2) and residual (F4) fractions were significantly different among treatments. The reducible V concentration (F2) in T3 (TiO_2+biochar-amended soil) was significantly lower than in the unamended soil (T4). Conversely, T3 (TiO_2+BC-amended soils) exhibited significantly higher V concentrations in the residual fraction (F4) than the other treatments. Approximately half of the total V content was found in the residual fraction, with 42% in the unamended soil (T4) and 58% in the TiO_2+BC-amended soil (T3).

3.4 | Characterization of Solid Materials After the Incubation Study

Mineralogical signatures of amended and unamended soil at the end of the incubation period showed dominant peaks indicating montmorillonite ($d = 1.39$ nm), illite ($d = 0.99$ nm), kaolinite ($d = 0.7$ nm), and quartz ($d = 0.33$ and 0.42 nm; Supporting Information S1: Figure 1). The mineralogical signatures of the soil did not change with the V contamination or by the addition of amendments. However, it should be noted that, with most laboratory-based X-ray instruments, only crystalline materials present at concentrations ~10–20 g kg^{-1} can be detected. Therefore, a more powerful X-ray absorption spectroscopy

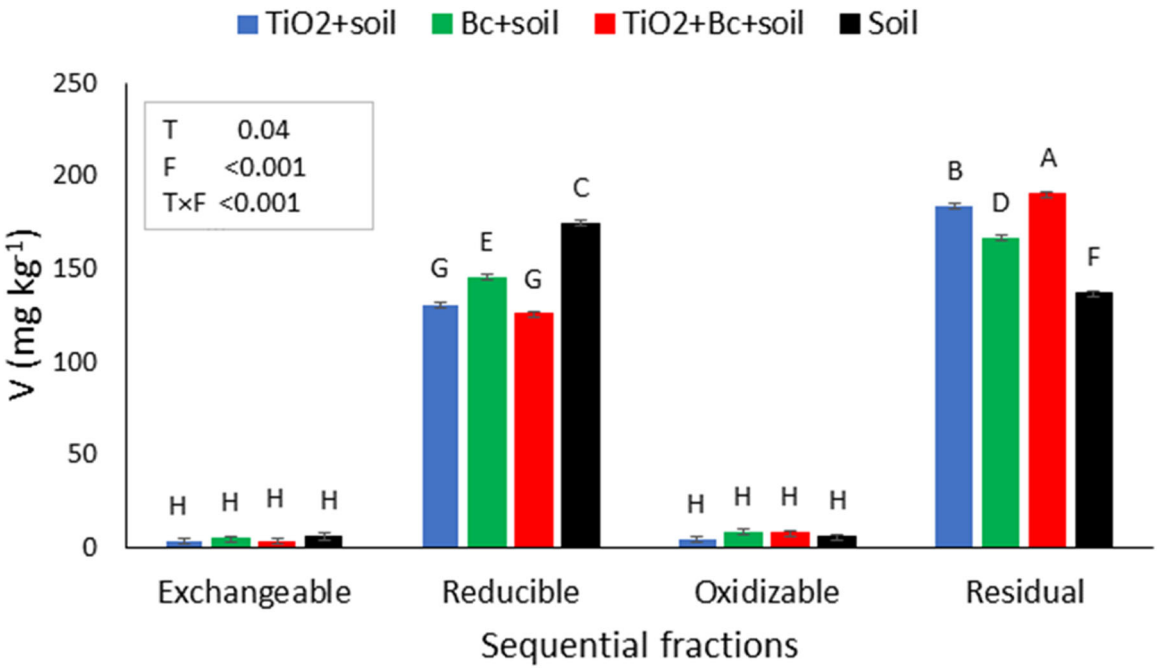

FIGURE 3 | Sequential fractions extracted from unamended soil and soil amended with TiO_2, biochar (Bc), and a mix of TiO_2 and Bc. The different uppercase letters (A–H) indicate Tukey's difference at a significance level of alpha = 0.05 (T = treatments, F = fractions). Error bars show the standard error. [Color figure can be viewed at wileyonlinelibrary.com]

(XAS) would be better suited to investigate the V species in soils (Shaheen et al. 2019).

The FTIR spectrum of nano-TiO_2 (Figure 4a) showed a broad absorption centered at ~3400 cm^{-1} and a narrower band at ~1625 cm^{-1} (Soria et al. 2007). The characteristic peak at 1625 cm^{-1} is attributed to Ti-O bond extension in anatase (Ma and Tu 2011). The stretching and bending peaks of FTIR spectra revealed several functional groups in biochar (Figure 4b). The broad peak at 3550–3200 cm^{-1} corresponds to the stretching vibration of hydrogen-bonded OH groups (Keiluweit et al. 2010; Yu et al. 2020). This peak indicates the presence of phenols, alcohols, and chemisorbed water. The peak was broad because of the complex vibrational modes due to the mixed stretching vibration bands of the –OH group in hydrogen bonding and chemisorbed water (Shi et al. 2009; Luo et al. 2017). The sharp peak at 1633 cm^{-1} is due to aromatic C=C stretches (Cheng et al. 2006; Xiu et al. 2020), and the broad peak at 1439 cm^{-1} is due to the aromatic C–C bending (Rodríguez-Vila et al. 2018; Yu et al. 2020; Liu, He, and Uchimiya 2015). The broad peak at 1030 cm^{-1} is due to symmetric C–O stretching due to cellulose, hemicellulose, and lignin (Liu, He, and Uchimiya 2015). Therefore, the wood biochar consists of phenolic, alcoholic, aromatic (C=C and C–C), and C–O functional groups from cellulose, hemicellulose, and lignin compounds.

The FTIR spectra of T1 (TiO_2 + soil), T2 (biochar + soil), T3 (TiO_2 + biochar + soil), and T4 (soil only) are shown in Figure 5. A single distinctive peak at 3695 cm^{-1} indicates the Al–OH–Al stretch due to the presence of kaolinite (Singh, Fang, and Johnston 2016), while a single very sharp band observed at 3620 cm^{-1} followed by broadband around 3430 cm^{-1} assigned to OH stretching of structural OH groups and water in the mineral, characteristic to the expanding type clay mineral of montmorillonite (Reddy et al. 2017). FTIR spectra in the lower region show peaks mainly due to the vibrational modes of the SiO_4 tetrahedron (Reddy et al. 2017). Hydrated phyllosilicates (e.g., chlorite, illite, smectite) show peaks around 1630 cm^{-1}, related to the H–O–H bonds of absorbed water. These peaks, however, are not diagnostic features of specific clay minerals, but indicative of the presence of water-absorbed minerals like montmorillonite. Therefore, the dominant clay mineralogy of the soil is montmorillonite with a small amount of kaolinite. The addition of nano-TiO_2 or biochar did not alter these peaks.

4 | Discussion

4.1 | Adsorption of Vanadium Onto Soils With and Without Amendments

Our findings corroborate previous studies that demonstrated the dependency of pH and total V concentration on the adsorption of V onto colloidal surfaces (Luo et al. 2017, Larsson, Hadialhejazi, and Gustafsson 2017; Vessey et al. 2020). The desorption of V increases as pH increases because functional groups such as hydroxyl and carboxyl groups become deprotonated, which changes the soil colloid surface charge from positive to negative causing electrostatic repulsion of vanadate species (Chen et al. 2021). This matches the results of the adsorption edge experiment as adsorbed V began to noticeably decline after pH 5 due to increasing vanadate species. Beyond pH 6 the negative charge of the surface of nano-TiO_2 becomes unfavorable to vanadate adsorption, as illustrated by the steep decline in adsorbed V from pH 6 to 10. Predicted V speciation also showed above pH 6, approximately 60% of the V is present in polyvanadate forms

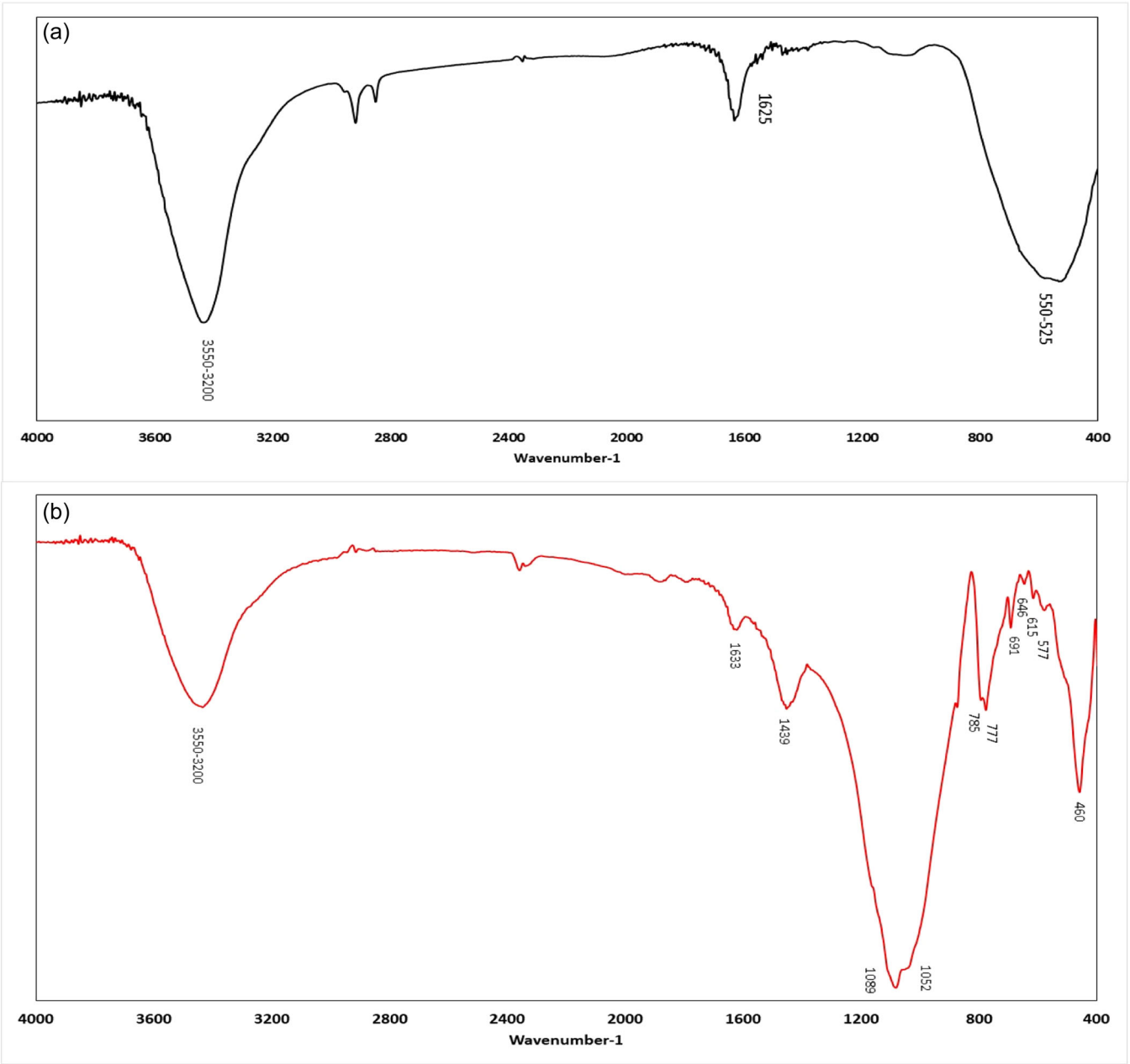

FIGURE 4 | Fourier transform infrared patterns in TiO_2 nanoparticles (a) and biochar (b) pure samples. [Color figure can be viewed at wileyonlinelibrary.com]

($H_2V_2O_7^{2-}$ and $V_4O_{12}^{-4}$) and ~35% as $H_2VO_4^-$ at a total V of 3924 μM. Therefore, the V speciation also may have contributed to the declining V adsorption at higher pH levels.

Soil amended with biochar+TiO_2 (T3) increased pH adsorption edge by 1 pH unit compared to the unamended control (T4). Further, the combined treatment achieved a total of 20% increase in V adsorption at the soil's natural pH. This was superior to the adsorption increased by the TiO_2 (7%) or biochar (4%), only treatments. It is possible that the mixture of nano-TiO_2 and biochar in T3 has a higher surface area and therefore provides numerous adsorption sites in comparison to T1 and T2, alone. The incorporation of nano-TiO_2 into biochar may increase the formation of inner-sphere complexes, thus increasing the adsorption efficiency of the soil as pH increases compared to either amendment alone.

4.2 | Distribution of Vanadates in the Soil Matrix of Amended and Unamended Soils

The experimental soil was alkaline, calcareous, and with a high organic matter content. This suggests that $H_2VO_4^-$ and HVO_4^{2-} (vanadates) species are the dominant V species in the soil environment due to the alkaline pH of the soil (Huang et al. 2015). Vanadium has a strong affinity toward soil colloids, including SOM, clay, and Fe/Al hydr(oxide) minerals (Mikkonen and Tummavuori 1994; Vessey et al. 2020). Natural soil colloids, such as biotite, kaolinite, calcite, and quartz, exhibit V retention in soils, mainly attributed to the complexation by active carboxylate and alcohol groups of colloidal components (Luo et al. 2017). XRD spectra revealed the presence of different minerals in natural soil colloids, including montmorillonite, kaolinite, illite, and quartz, which might contribute to

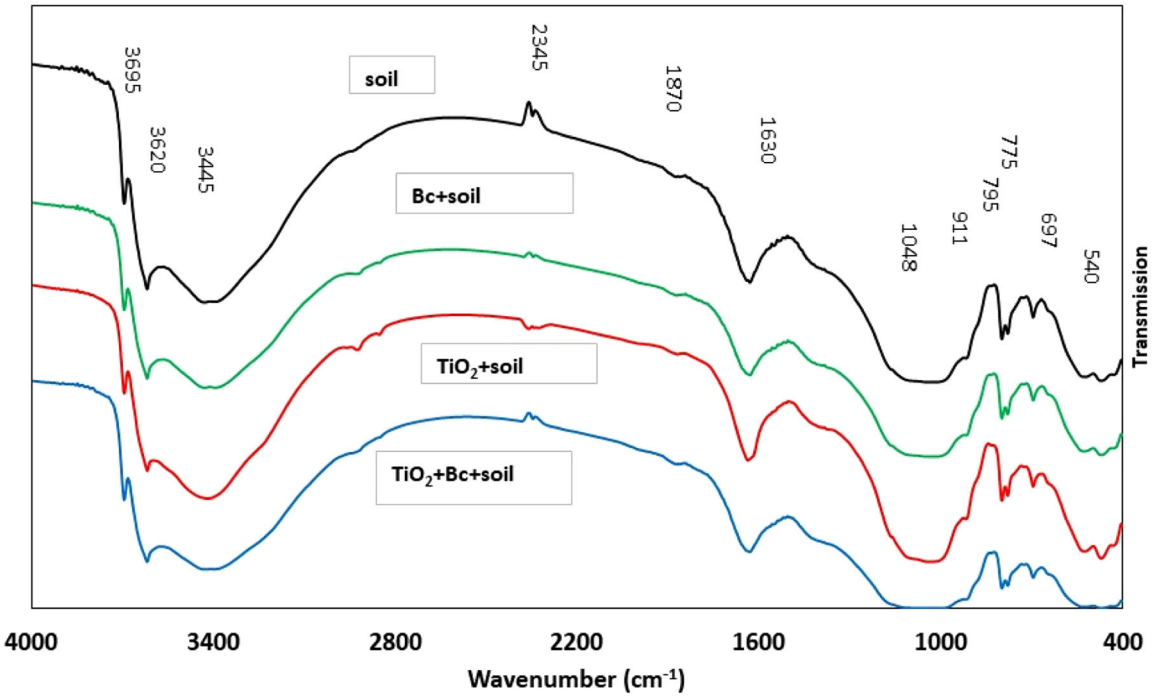

FIGURE 5 | Fourier transform infrared patterns of unamended soil and soil amended with TiO_2, biochar (Bc), and a mix of TiO_2 and Bc. [Color figure can be viewed at wileyonlinelibrary.com]

the sorption process. XANES spectroscopy at the V K-edge conducted on three chosen soils confirmed that the introduced vanadate primarily accumulated as adsorbed vanadate on Fe and Al hydrous oxides (Larsson, Hadialhejazi, and Gustafsson 2017). Given this, with the inclusion of TiO_2 as an amendment, an increased adsorption of V^{5+} can be anticipated, consistent with the findings of the present study.

Since vanadium exists as vanadate species such as $H_2VO_4^-$ and HPO_4^{2-} above pH 5, the electrostatic adsorption onto nano-TiO_2 should be favorable up to pH 5 (Reijonen, Metzler, and Hartikainen 2016). As adsorption occurs on the surface of nano-TiO_2 beyond the point of zero charge (pH_{pzc}), even in the presence of vanadate as the predominant V species, it indicates that the adsorption mechanism involves more than electrostatic interactions alone. There appears to be a covalent interaction between nano-TiO_2 and vanadate occurring between the positively charged titanium (Ti) sites and the negatively charged oxygen atoms on the vanadate. However, the increasing surface charge of any of the treatments will result in electrostatic repulsion of vanadate species, which decreases the probability of vanadate meeting the surface of either nano-TiO_2 or biochar. The T3 treatment showed the best V adsorption capacity at pH > 4.6 and had a considerably higher V adsorption at alkaline pH compared to other treatments. Maximum adsorption of V^{5+} occurred at pH ~4, where 70%–80% of the added V was retained by soils (Mikkonen and Tummavuori 1994). Naeem, Westerhoff, and Mustafa (2007) also found that V adsorption decreases with increasing pH, with maximum adsorption capacities achieved at pH 3–4 on Ti and Fe-based oxides.

The FTIR analysis of biochar indicated that the surface contained hydroxyl, carboxyl, and carbonyl groups which provide oxygen for vanadate to bond to, while nano-TiO_2 provides Ti^{+2}, oxygen, and hydroxyl groups to bond with vanadate. The pH_{pzc} of anatase (TiO_2 polymorph) is 6.42 and, therefore, the V adsorption efficiency due to electrostatic attraction is decreased at higher pH (Ma and Tu 2011). At alkaline pH, as of the experimental soil, OH^- exerts a competitive effect on the adsorption of vanadate onto TiO_2 (Naeem, Westerhoff, and Mustafa 2007; Yin et al. 2018; Wołowicz et al. 2022). The surface of TiO_2 contains abundant bridging and terminal –OH groups, which can be complex with V species via hydrogen bonds or participate in a bidentate bond with two metal sites (Yin et al. 2018; Naeem, Westerhoff, and Mustafa 2007). Other researchers (Vessey et al. 2020; Abernathy et al. 2021) revealed the formation of inner-sphere complexes and bidentate-mononuclear edge-sharing complexes between V^{5+} and oxide surfaces in soils. Abernathy et al. (2022) showed the possibility of V^{5+} adsorption onto surfaces with terminal −OH and metal–O groups, implicating the contribution of varied mineral surfaces to the adsorption of V^{5+} in terrestrial and aquatic systems. Therefore, the interaction mechanisms between TiO_2 and V could be the combination of electrostatic attraction, H-bonding, and the formation of inner-sphere complexes between TiO_2 and vanadates. Biochar possesses several functional groups, such as carbonyl, carboxyl, hydroxyl, and phenolic groups, which can act in various ways to immobilize V, either by complexation, electrostatic interactions, or reduction (Namasivayam and Sangeetha 2006; Yu et al. 2020; El-Naggar et al. 2021).

Among the four fractions of V, the acid-soluble (exchangeable) portion is considered highly mobile, while their reducible and oxidizable parts are assumed to be relatively stable under normal conditions (Song et al. 2018). Therefore, the sum of the acid-soluble, reducible, and oxidizable fractions is considered bioavailable (Zeng et al. 2011). Even though exchangeable fractions (F1) were not significantly different among

treatments, the combined biochar+nano-TiO_2 showed 44% less V than that of unamended soil. The residual fraction of the V consists of ~42%–58% of the total V in all treatments. Typically, the majority of V in the soil is contained in the residual fraction, which consists of the mineral phases that are difficult to break down; therefore, the majority of V is not usually mobile in soil (Huang et al. 2015; Reijonen, Metzler, and Hartikainen 2016). Other findings also suggest that over 50% of the V in the soil is typically associated with the residual fraction (Teng et al. 2011; Cappuyns and Swennen 2014). The fractionation study revealed that the F2 or the reducible fraction was significantly decreased by the application of nano-TiO_2+biochar (T3) compared to unamended soil (T4). The residual fraction (F4) in T3 was significantly higher than in T4 (soil); therefore, T3 (1% w/w nano-TiO_2+5% biochar) was the most successful in transforming mobile and potentially mobile V into immobile V in the residual fraction (F4). Additional research is required to elucidate the specific forms of vanadium present within the operationally defined fractions in soils. These studies would contribute to a deeper understanding of the distribution, mobility, and potential environmental impact of vanadium in soil systems.

5 | Conclusions

It is worth noting that soil V^{5+} has high bioavailability, creating a significant environmental problem, and necessitating urgent remediation of V-contaminated soils, especially under neutral to alkaline conditions. The adsorption edge experiment revealed that the mixture of nano-TiO_2 and biochar was better suited for V adsorption at alkaline pH. This could be attributed to the increase in adsorption sites on the biochar by nano-TiO_2 and a stronger complex formed between vanadate ions and the nano-TiO_2 surface. Biochar contains OH, C═O, C–O, and C═C groups and, therefore, adsorption of V facilitated by inner-sphere complexation with π-bonded or aromatic carbon or electrostatic interactions between vanadate and the oxygen or hydroxyl groups. To further support this hypothesis, the fractionation of V revealed that a mixed amendment significantly reduced the mobile fraction of V in the soil compared to unamended soil and increased the residual fraction of V. This suggests that the application of 1% w/w nano-TiO_2 + 5% biochar can adsorb V so that its mobility declines and prevents it from becoming potentially mobile in contaminated soil. A field validation study would be appropriate before making recommendations for remediating V using TiO_2 and biochar amendments, as field conditions are difficult to replicate accurately in laboratory studies due to significant changes in temperature, moisture, and oxygen levels.

Acknowledgments

The authors acknowledge Neepin Cook, Kaydon Laurin, and Chathuri Mudalige for technical assistance. This research was financially supported by the Natural Sciences and Engineering Research Council of Canada—Discovery Development Grant (NSERC-DDG, S.P. Indraratne).

Conflicts of Interest

The authors declare no conflicts of interest.

References

Abernathy, M. J., M. V. Schaefer, R. Ramirez, et al. 2022. "Vanadate Retention by Iron and Manganese Oxides." *ACS Earth and Space Chemistry* 6, no. 8: 2041–2052.

Abernathy, M. J., M. V. Schaefer, C. J. Vessey, H. Liu, and S. C. Ying. 2021. "Oxidation of V (IV) by Birnessite: Kinetics and Surface Complexation." *Environmental Science & Technology* 55, no. 17: 11703–11712.

Ahmad, Z., B. Gao, A. Mosa, et al. 2018. "Removal of Cu(II), Cd(II), and Pb(II) Ions From Aqueous Solutions by Biochars Derived From Potassium-Rich Biomass." *Journal of Cleaner Production* 180: 437–449.

Cappuyns, V., and R. Swennen. 2014. "Release of Vanadium From Oxidized Sediments: Insights From Different Extraction and Leaching Procedures." *Environmental Science and Pollution Research* 21: 2272–2282.

Chen, L., J. Liu, W. Hu, J. Gao, and J. Yang. 2021. "Vanadium in Soil-Plant System: Source, Fate, Toxicity, and Bioremediation." *Journal of Hazardous Materials* 405: 124200. https://doi.org/10.1016/j.jhazmat.2020.124200.

Cheng, C. H., J. Lehmann, J. E. Thies, S. D. Burton, and M. H. Engelhard. 2006. "Oxidation of Black Carbon by Biotic and Abiotic Processes." *Organic Geochemistry* 37, no. 11: 1477–1488.

Crans, D. C., J. J. Smee, E. Gaidamauskas, and L. Yang. 2004. "The Chemistry and Biochemistry of Vanadium and the Biological Activities Exerted by Vanadium Compounds." *Chemical Reviews* 104: 849–902. https://doi.org/10.1021/cr020607t.

El-Naggar, A., S. M. Shaheen, S. X. Chang, D. Hou, Y. S. Ok, and J. Rinklebe. 2021. "Biochar Surface Functionality Plays a Vital Role in Immobilization and Phytoavailability of Soil Vanadium." *ACS Sustainable Chemistry & Engineering* 9: 6864–6874.

Fei, Y., B. Zhang, J. He, C. Chen, and H. Liu. 2022. "Dynamics of Vertical Vanadium Migration in Soil and Interactions With Indigenous Microorganisms Adjacent to Tailing Reservoir." *Journal of Hazardous Materials* 424: 127608.

Gäbler, H. E., K. Glüh, A. Bahr, and J. Utermann. 2009. "Quantification of Vanadium Adsorption by German Soils." *Journal of Geochemical Exploration* 103, no. 1: 37–44.

Gan, C., M. Liu, J. Lu, and J. Yang. 2020. "Adsorption and Desorption Characteristics of Vanadium (V) on Silica." *Water, Air, & Soil Pollution* 231: 1–11.

Ghanim, B., J. G. Murnane, L. O'Donoghue, R. Courtney, J. T. Pembroke, and T. F. O'Dwyer. 2020. "Removal of Vanadium From Aqueous Solution Using a Red Mud Modified Saw Dust Biochar." *Journal of Water Process Engineering* 33: 101076.

Gustafsson, J. P. 2013. *Visual MINTEQ—Visual MINTEQ—A Free Equilibrium Speciation Model*. https://vminteq.lwr.kth.se/. (visited July, 2023).

Gustafsson, J. P. 2019. "Vanadium Geochemistry in the Biogeosphere—Speciation, Solid-Solution Interactions, and Ecotoxicity." *Applied Geochemistry* 102: 1–25. https://doi.org/10.1016/j.apgeochem.2018.12.027.

Haak, M. R., and S. P. Indraratne. 2023. "Soil Amendments for Vanadium Remediation: A Review of Remediation of Vanadium in Soil Through Chemical Stabilization and Bioremediation." *Environmental Geochemistry and Health* 45: 4107–4125. https://doi.org/10.1007/s10653-023-01498-8.

He, L., H. Zhong, G. Liu, Z. Dai, P. C. Brookes, and J. Xu. 2019. "Remediation of Heavy Metal Contaminated Soils by Biochar: Mechanisms, Potential Risks and Applications in China." *Environmental Pollution* 252: 846–855.

Hu, Q., Z. Xiao, X. Xiong, G. Zhou, and X. Guan. 2015. "Predicting Heavy Metals' Adsorption Edges and Adsorption Isotherms on MnO_2 With the Parameters Determined From Langmuir Kinetics." *Journal of Environmental Sciences* 27: 207–216.

Hu, X., Y. Yue, and X. Peng. 2018. "Release Kinetics of Vanadium From Vanadium (III, IV, and V) Oxides: Effect of pH, Temperature, and Oxide

Dose." *Journal of Environmental Sciences* 67: 96–103. https://doi.org/10.1016/j.jes.2017.08.006.

Huang, J. H., F. Huang, L. Evans, and S. Glasauer. 2015. "Vanadium: Global (Bio)Geochemistry." *Chemical Geology* 417: 68–89. https://doi.org/10.1016/j.chemgeo.2015.09.019.

Imtiaz, M., M. S. Rizwan, S. Xiong, et al. 2015. "Vanadium, Recent Advancements and Research Prospects: A Review." *Environment International* 80: 79–88.

Indraratne, S. P., G. M. Pierzynski, L. R. Baker, and P. V. Vara Prasad. 2021. "Nano-Oxides Immobilize Cadmium, Lead, and Zinc in Mine Spoils and Contaminated Soils Facilitating Plant Growth." *Canadian Journal of Soil Science* 101: 543–554. https://doi.org/10.1139/CJSS-2020-0127.

Keiluweit, M., P. S. Nico, M. G. Johnson, and M. Kleber. 2010. "Dynamic Molecular Structure of Plant Biomass-Derived Black Carbon (Biochar)." *Environmental Science & Technology* 44, no. 4: 1247–1253.

Khan, S., T. G. Kazi, N. F. Kolachi, et al. 2011. "Hazardous Impact and Translocation of Vanadium (V) Species From Soil to Different Vegetables and Grasses Grown in the Vicinity of Thermal Power Plant." *Journal of Hazardous Materials* 190: 738–743. https://doi.org/10.1016/j.jhazmat.2011.03.105.

Kollur, S. P., and U. R. Shwetha. 2020. "Potential Medicinal Applications of Vanadium and Its Coordination in Current Research Prospects: A Review." *Current Bioactive Compounds* 16(3): 201–209. https://doi.org/10.2174/1573407214666181115111357.

Larsson, M. A., G. Hadialhejazi, and J. P. Gustafsson. 2017. "Vanadium Sorption by Mineral Soils: Development of a Predictive Model." *Chemosphere* 168: 925–932.

Liu, L., W. Li, W. Song, and M. Guo. 2018. "Remediation Techniques for Heavy Metal-Contaminated Soils: Principles and Applicability." *Science of the Total Environment* 633: 206–219. https://doi.org/10.1016/j.scitotenv.2018.03.161.

Liu, Y., Z. He, and M. Uchimiya. 2015. "Comparison of Biochar Formation From Various Agricultural By-Products Using FTIR Spectroscopy." *Modern Applied Science* 9, no. 4: 246.

Lomaglio, T., N. Hattab-Hambli, F. Miard, et al. 2018. "Cd, Pb, and Zn Mobility and Bioavailability in Contaminated Soils From a Former Smelting Site Amended With Biochar." *Environmental Science and Pollution Research* 25: 25744–25756.

Lu, X., W. D. Johnson, and J. Hook. 1998. "Reaction of Vanadate With Aquatic Humic Substances: An ESR and 51 V NMR Study." *Environmental Science & Technology* 32, no. 15: 2257–2263.

Luo, X., L. Yu, C. Wang, et al. 2017. "Sorption of Vanadium (V) Onto Natural Soil Colloids Under Various Solution pH and Ionic Strength Conditions." *Chemosphere* 169: 609–617.

Ma, L., and S. X. Tu. 2011. "Removal of Arsenic From Aqueous Solution by Two Types of Nano TiO_2 Crystals." *Environmental Chemistry Letters* 9: 465–472.

MAFRI. 2010. "Manitoba Agriculture and Rural Initiative." Soil Series Descriptions. http://www.gov.mb.ca/agriculture/land/soil-survey/pubs/description_of_soil_series_in_mb.pdf.

Makhotkina, E. S., and M. V. Shubina. 2017. "Industrial, Ecological and Resource-Efficient Aspects of Vanadium Production and Use of Technogenic Vanadium Sources." *Solid State Phenomena* 265: 994–998.

Mehmood, S., M. Rizwan, S. Bashir, et al. 2018. "Comparative Effects of Biochar, Slag, and Ferrous–Mn Ore on Lead and Cadmium Immobilization in Soil." *Bulletin of Environmental Contamination and Toxicology* 100: 286–292.

Mikkonen, A., and J. Tummavuori. 1994. "Retention of Vanadium (V) by Three Finnish Mineral Soils." *European Journal of Soil Science* 45, no. 3: 361–368.

Molina, M., F. Aburto, R. Calderón, M. Cazanga, and M. Escudey. 2009. "Trace Element Composition of Selected Fertilizers Used in Chile: Phosphorus Fertilizers as a Source of Long-Term Soil Contamination." *Soil and Sediment Contamination: An International Journal* 18: 497–511. https://doi.org/10.1080/15320380902962320.

Naderi Peikam, E., and M. Jalali. 2019. "Application of Three Nanoparticles (Al_2O_3, SiO_2 and TiO_2) for Metal-Contaminated Soil Remediation (Measuring and Modeling)." *International Journal of Environmental Science and Technology* 16: 7207–7220.

Naeem, A., P. Westerhoff, and S. Mustafa. 2007. "Vanadium Removal by Metal (Hydr)Oxide Adsorbents." *Water Research* 41: 1596–1602. https://doi.org/10.1016/j.watres.2007.01.002.

Namasivayam, C., and D. Sangeetha. 2006. "Removal and Recovery of Vanadium (V) by Adsorption Onto $ZnCl_2$ Activated Carbon: Kinetics and Isotherms." *Adsorption* 12: 103–117. https://doi.org/10.1007/s10450-006-0373-3.

Peacock, C. L., and D. M. Sherman. 2004. "Vanadium (V) Adsorption Onto Goethite (α-FeOOH) at pH 1.5 to 12: A Surface Complexation Model Based on Ab Initio Molecular Geometries and EXAFS Spectroscopy." *Geochimica et Cosmochimica Acta* 68: 1723–1733.

Pueyo, M., J. Mateu, A. Rigol, M. Vidal, J. F. López-Sánchez, and G. Rauret. 2008. "Use of the Modified BCR Three-Step Sequential Extraction Procedure for the Study of Trace Element Dynamics in Contaminated Soils." *Environmental Pollution* 152, no. 2: 330–341.

Reddy, R. T., S. Kaneko, T. Endo, and S. Lakshmi Reddy. 2017. "Spectroscopic Characterization of Bentonite." *Journal of Lasers, Optics and Photonics* 4, no. 3. https://doi.org/10.4172/2469-410X.1000171.

Reijonen, I., M. Metzler, and H. Hartikainen. 2016. "Impact of Soil pH and Organic Matter on the Chemical Bioavailability of Vanadium Species: The Underlying Basis for Risk Assessment." *Environmental Pollution* 210: 371–379. https://doi.org/10.1016/j.envpol.2015.12.046.

Rodríguez-Vila, A., H. Selwyn-Smith, L. Enunwa, I. Smail, E. F. Covelo, and T. Sizmur. 2018. "Predicting Cu and Zn Sorption Capacity of Biochar From Feedstock C/N Ratio and Pyrolysis Temperature." *Environmental Science and Pollution Research* 25: 7730–7739.

SAS Institute Inc. 2013. *SAS/STAT User's Guide version 9.4*. Statistical Analysis System (SAS Institute Inc).

Shaheen, S. M., D. S. Alessi, F. M. G. Tack, et al. 2019. "Redox Chemistry of Vanadium in Soils and Sediments: Interactions With Colloidal Materials, Mobilization, Speciation, and Relevant Environmental Implications—A Review." *Advances in Colloid and Interface Science* 265: 1–13. https://doi.org/10.1016/j.cis.2019.01.002.

Shi, T., S. Jia, Y. Chen, et al. 2009. "Adsorption of Pb (II), Cr (III), Cu (II), Cd (II) and Ni (II) Onto a Vanadium Mine Tailing From Aqueous Solution." *Journal of Hazardous Materials* 169, no. 1–3: 838–846.

Singh, B., Y. Fang, and C. T. Johnston. 2016. "A Fourier-Transform Infrared Study of Biochar Aging in Soils." *Soil Science Society of America Journal* 80, no. 3: 613–622.

Song, Z., L. Dong, B. Shan, and W. Tang. 2018. "Assessment of Potential Bioavailability of Heavy Metals in the Sediments of Land-Freshwater Interfaces by Diffusive Gradients in Thin Films." *Chemosphere* 191: 218–225.

Soria, J., J. Sanz, I. Sobrados, et al. 2007. "FTIR and NMR Study of the Adsorbed Water on Nanocrystalline Anatase." *Journal of Physical Chemistry C* 111, no. 28: 10590–10596.

Teng, Y., J. Yang, Z. Sun, J. Wang, R. Zuo, and J. Zheng. 2011. "Environmental Vanadium Distribution, Mobility and Bioaccumulation in Different Land-Use Districts in Panzhihua Region, SW China." *Environmental Monitoring and Assessment* 176: 605–620.

Vessey, C. J., M. P. Schmidt, M. Abdolahnezhad, D. Peak, and M. B. J. Lindsay. 2020. "Adsorption of (Poly) Vanadate Onto

Ferrihydrite and Hematite: An In Situ ATR–FTIR Study." *ACS Earth and Space Chemistry* 4, no. 4: 641–649.

Wanty, R. B., and M. B. Goldhaber. 1992. "Thermodynamics and Kinetics of Reactions Involving Vanadium in Natural Systems: Accumulation of Vanadium in Sedimentary Rocks." *Geochimica et Cosmochimica Acta* 56, no. 4: 1471–1483.

Weber, K., and P. Quicker. 2018. "Properties of Biochar." *Fuel* 217: 240–261.

Weidner, E., E. Karbassiyazdi, A. Altaee, T. Jesionowski, and F. Ciesielczyk. 2022. "Hybrid Metal Oxide/Biochar Materials for Wastewater Treatment Technology: A Review." *ACS Omega* 7: 27062–27078. https://doi.org/10.1021/acsomega.2c02909.

Wołowicz, A., M. Wawrzkiewicz, Z. Hubicki, K. Siwińska-Ciesielczyk, A. Kubiak, and T. Jesionowski. 2022. "Enhanced Removal of Vanadium (V) From Acidic Streams Using Binary Oxide Systems of TiO_2-ZrO_2 and TiO_2-ZnO Type." *Separation and Purification Technology* 280: 119916. https://doi.org/10.1016/j.seppur.2021.119916.

Xiao, L., D. Guan, M. R. Peart, Y. Chen, and Q. Li. 2017. "The Respective Effects of Soil Heavy Metal Fractions by Sequential Extraction Procedure and Soil Properties on the Accumulation of Heavy Metals in Rice Grains and Brassicas." *Environmental Science and Pollution Research* 24: 2558–2571.

Xiu, F. R., Y. Wang, X. Yu, et al. 2020. "A Novel Safety Treatment Strategy of DEHP-Rich Flexible Polyvinyl Chloride Waste Through Low-Temperature Critical Aqueous Ammonia Treatment." *Science of the Total Environment* 708: 134532.

Yin, X., X. Meng, Y. Zhang, et al. 2018. "Removal of V (V) and Pb (II) by Nanosized TiO_2 and ZnO From Aqueous Solution." *Ecotoxicology and Environmental Safety* 164: 510–519. https://doi.org/10.1016/j.ecoenv.2018.08.066.

Yu, Y., J. Li, Y. Liao, and J. Yang. 2020. "Effectiveness, Stabilization, and Potential Feasible Analysis of a Biochar Material on Simultaneous Remediation and Quality Improvement of Vanadium Contaminated Soil." *Journal of Cleaner Production* 277: 123506.

Zand, A. D., A. M. Tabrizi, and A. V. Heir. 2020. "Co-Application of Biochar and Titanium Dioxide Nanoparticles to Promote Remediation of Antimony From Soil by *Sorghum bicolor*: Metal Uptake and Plant Response." *Heliyon* 6, no. 8: e04669. DOI:10.1016/j.heliyon.2020.e04669.

Zeng, F., S. Ali, H. Zhang, et al. 2011. "The Influence of pH and Organic Matter Content in Paddy Soil on Heavy Metal Availability and Their Uptake by Rice Plants." *Environmental Pollution* 159: 84–91.

Zhang, B., L. Hao, C. Tian, et al. 2015. "Microbial Reduction and Precipitation of Vanadium (V) in Groundwater by Immobilized Mixed Anaerobic Culture." *Bioresource Technology* 192: 410–417.

Zhang, Y. M., S. X. Bao, T. Liu, T. J. Chen, and J. Huang. 2011. "The Technology of Extracting Vanadium From Stone Coal in China: History, Current Status and Future Prospects." *Hydrometallurgy* 109, no. 1–2: 116–124.

Supporting Information

Additional supporting information can be found online in the Supporting Information section.